

Impact of Tropical Disturbance on the Indian Summer Monsoon Onset Simulated by a Global Cloud-System-Resolving Model

Yoshiyuki Kajikawa¹, Tsuyoshi Yamaura¹, Hirofumi Tomita^{1,2}, and Masaki Satoh^{2,3}

¹*RIKEN Advanced Institute for Computational Science, Kobe, Japan*

²*Japan Agency for Marine-Earth Science and Technology, Yokohama, Japan*

³*Atmosphere and Ocean Research Institute, The University of Tokyo, Kashiwa, Japan*

Abstract

The onset of the Indian summer monsoon (ISM) in 2012 was investigated using the nonhydrostatic icosahedral atmospheric model (NICAM), a global cloud-system resolving model. We focused on the effect of tropical disturbances on ISM onset and considered the potential extension of onset predictability. A series of NICAM experiments was performed under various initial conditions for the period 10 May to 10 June, 2012. NICAM showed promising performance by realistically simulating ISM onset based on the initial conditions two weeks before the onset. ISM onset in both observations and simulations was accompanied by northward-migrating tropical disturbances over the Bay of Bengal and the Arabian Sea. These disturbances were generated by the eastward propagating disturbance along the equatorial Indian Ocean. As indicated by a comparison of NICAM experimental results with those obtained by the Japan Meteorological Agency Operational Ensemble Prediction System, we suggest that the better reproducing the tropical disturbance enhances the potential to extend the predictability of the transition phase in the Asian summer monsoon.

(Citation: Kajikawa, Y., T. Yamaura, H. Tomita, and M. Satoh, 2015: Impact of tropical disturbance on the Indian summer monsoon onset simulated by a global cloud-system-resolving model. *SOLA*, **11**, 80–84, doi:10.2151/sola.2015-020.)

1. Introduction

The onset of the Indian summer monsoon (ISM) signifies the commencement of the rainy season in south-southeastern Asia, with an abrupt change in large-scale atmospheric circulations (Joseph et al. 1994; Joseph et al. 2006). The interannual variability in the timing of ISM onset has marked effects on agricultural and economic practices in India and the broad Asian monsoon area (Gadgil and Rupa Kumar 2006). This interannual variability of the onset is not always correlated with that of the seasonal mean monsoon strength during boreal summer (Moron and Robertson 2014). For instance, ISM onset was two weeks earlier in 1989 than in 2003, despite similar seasonal mean ISM strengths for the two years (Subrahmanyam et al. 2013).

The variability in seasonal mean monsoon strength has been understood as a boundary value problem, e.g. the impact of sea surface temperature (SST) anomalies associated with the El Niño–Southern Oscillation (Kirtman and Shukla 2000). In contrast, as part of the seasonal transition, monsoon onset is reported as a complex event that involves a combination of several effects: increased thermal contrast between land and ocean, increased convective instability, and the arrival of tropical disturbances (e.g., Madden Julian oscillation (MJO), tropical cyclones, and tropical depressions) (Hung and Yanai 2004). Thus, the onset of monsoon conditions can be markedly affected not only by the boundary conditions but also by internal variability, such as tropical disturbances. In fact, ISM onset evolution is often associated with the

first arrival of northward-propagating intraseasonal variability (ISV). Therefore, the arrival of the tropical disturbance may be the more dominant effect in ISM initiation.

Recently, the global climate modeling has been advanced for the better simulation of Asian summer monsoon in many aspects; climatological seasonal mean, annual cycle, interannual variability and intraseasonal variability (Sperber et al. 2013). However, using the global model to predict the timing of ISM onset remains a challenging issue (Li and Zhang 2009). In general, ISM onset in global model simulations is much later than its actual occurrence (Sperber et al. 2013). Thus, the conditions for ISM initiation must be identified to improve the predictability and reproducibility of tropical disturbances in model simulations.

In this study, we investigated the conditions for ISM onset in 2012 as a normal year, using the nonhydrostatic icosahedral atmospheric model (NICAM), a global cloud-system model without convective parameterization, and considered potential extension of ISM onset predictability. This model is able to simulate tropical disturbances better, in particular, the MJO (Miyakawa et al. 2014). NICAM simulations were compared with other operational models to identify the precursor signals for ISM onset, which was resolved in NICAM simulations.

This paper is organized as follows. In Section 2, datasets are presented along with a description of the model and our experimental design. NICAM simulation results are examined and compared with observational data in Section 3. The proposed model is then compared with conventional models in Section 4, followed by concluding remarks.

2. Models and datasets

This study used wind field data from the Japan 25-year Reanalysis (JRA-25)/Japan Meteorological Agency (JMA) Climate Data Assimilation System (JCDAS) reanalysis (Onogi et al. 2007) and daily mean-interpolated outgoing longwave radiation (OLR) data from a National Oceanic and Atmospheric Association (NOAA) satellite (Liebmann and Smith 1996), as the observational dataset. A global cloud-system resolving model based on NICAM (grid spacing: 14 km; vertical levels: 38) was used for ISM onset simulations. NICAM was developed by (Satoh et al. 2008; Tomita and Satoh 2004); an overview of NICAM research and the current status of development are described in (Satoh et al. 2014). Previous studies have demonstrated the superior performance of NICAM in its ability to predict tropical disturbances, such as tropical cyclones (Fudeyasu et al. 2008; Nakano et al. 2015; Yamaura et al. 2013) and MJO (Miura et al. 2007; Miyakawa et al. 2014), as opposed to conventional general circulation models (GCMs). Thus, the proposed model presented in this study is expected to improve the predictability of ISM onset, particularly with tropical disturbance origins. Note that cumulus parameterization was not considered in this study (see (Holloway et al. 2013) and cloud processes were explicitly calculated using cloud microphysics.

To capture ISM onset and examine its sensitivity to the initial conditions, a series of experiments with different initial conditions was performed. The simulation started at 00 UTC each day during the period examined, from 10 May, 2012 to 10 June, 2012. The earliest initial date was more than three weeks prior to the ISM

onset in 2012. Time integration was performed for 30 days in each simulation. The initial atmospheric conditions were based on JMA grid point value (GPV) analysis data from a global spectral model. The initial oceanic conditions were based on a dataset finalized by the National Centers for Environmental Prediction. We prepared long-term spin-up data, using low-resolution NICAM (the equivalent of a 224-km mesh) and applied these data to initial land conditions. The nudged SST and weekly NOAA SST (Reynolds et al. 2002) were used for time-varying boundary conditions.

To evaluate the performance of the NICAM simulations, we also used the one-month forecast of the JMA Ensemble Prediction System (EPS). The initial conditions of the JMA EPS are shifted by 7 days. The global model for predictions has a horizontal grid spacing of 0.5625 deg (TL319; equivalent to 60 km) and 60 vertical levels. Each global analysis output consists of 25 ensemble members with perturbations. We recall the cases of 17 May and 23 May as they relate to ISM onset in 2012 and compare these data with NICAM simulations.

3. Observation and simulation of ISM onset

The announcement of ISM onset in 2012 over Kerala by the Indian Institute of Tropical Meteorology occurred on 5 June. Because this date is close to the climatological mean ISM onset date of 1 June, we considered the ISM onset of 2012 to be a normal event in terms of annual occurrence. In this study, we used the ISM index defined by (Wang et al. 2001), the meridional shear of the zonal wind at 850 hPa over the Indian continent ($40^{\circ}\text{E}-80^{\circ}\text{E}$, $5^{\circ}\text{N}-15^{\circ}\text{N}$ minus $70^{\circ}\text{E}-90^{\circ}\text{E}$, $20^{\circ}\text{N}-30^{\circ}\text{N}$). Figure 1 shows the time series of ISM index observations and NICAM simulations. The observational ISM index (thick red line) turned positive, indicating westerly wind shear, from 24 May to 1 June. This signified ISM onset of large-scale circulation in 2012. This change in the wind circulation brought about an increase in precipitation over the Indian sub-continent and the commencement of the rainy season. It is noteworthy that the NICAM simulations initialized in mid-May show an abrupt onset of the monsoon, quite similar to observations. Because the simulations initialized before 14 May had a less abrupt change in wind circulation during late-May, we assumed that the initial conditions after 15 May would

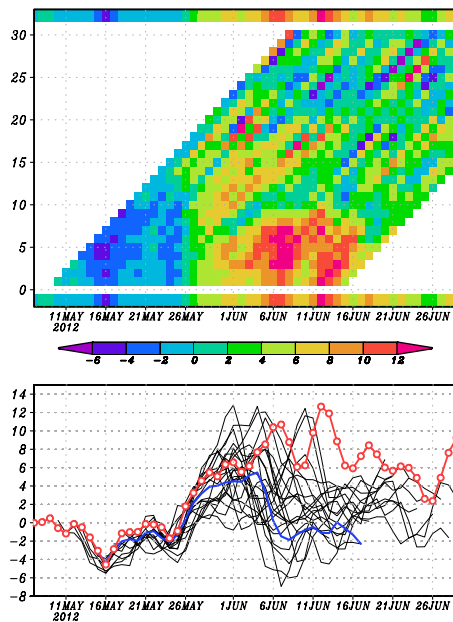


Fig. 1. (Top) Time-integrated time (day) diagram of the Indian summer monsoon (ISM) indices. Top and bottom shading denote the observational ISM index. Each simulated ISM index goes upper right. (Bottom) Time series of the ISM indices for each run (black), averaging five members with initial conditions covering 15–19 May (blue) and actual observations (red).

be sufficient for more realistic ISM onset simulations. The initial conditions of five ensemble members corresponding to 15–19 May 2012 were used for analyses in this study. The lead time for abrupt ISM onset prediction was approximately two weeks.

The ISM index of the NICAM simulations reached nearly zero in the middle of June, exhibiting tendencies that drifted from observational features. Although this behavior was the result of northward-shifted of the monsoon westerly axis, we confirmed that the simulated ISM became established after monsoon the onset in early June, with increasing rainfall over the Indian sub-continent. In addition, NICAM simulations have had difficulty in providing an accurate representation of the western North Pacific monsoon (WNPM). In fact, the WNPM index defined by (Wang et al. 2001) strays from that observed after 4–5 days integration during late May and early June (Figure not shown). The lead time for the prediction is also much less than that of ISM onset; this is due to relatively weak convection over the western North Pacific area compared with observations, similar to previous NICAM simulations (Oouchi et al. 2009).

Figures 2 and 3 show the evolution of ISM onset in observations and NICAM simulations, averaging five runs with different initial conditions over the period from 15–19 May, 2012. In the observations, the enhanced convection located over the south-eastern Indian Ocean on 21 May is thought to be eastward propagating convection system from the western Indian Ocean. The Boreal Summer Intraseasonal Oscillation (BSISO) index (Kikuchi et al. 2012) indicates that the convection was associated with the intraseasonal variability over the India and Maritime continent. From 23 May through 27 May, twin cyclonic circulations formed along the 90°E gridline in the northern and southern hemispheres, and the westerly wind along the equator strengthened. From 23 May to 31 May, convection with a positive vortex over the Bay of Bengal increased in strength and moved northward. This induced

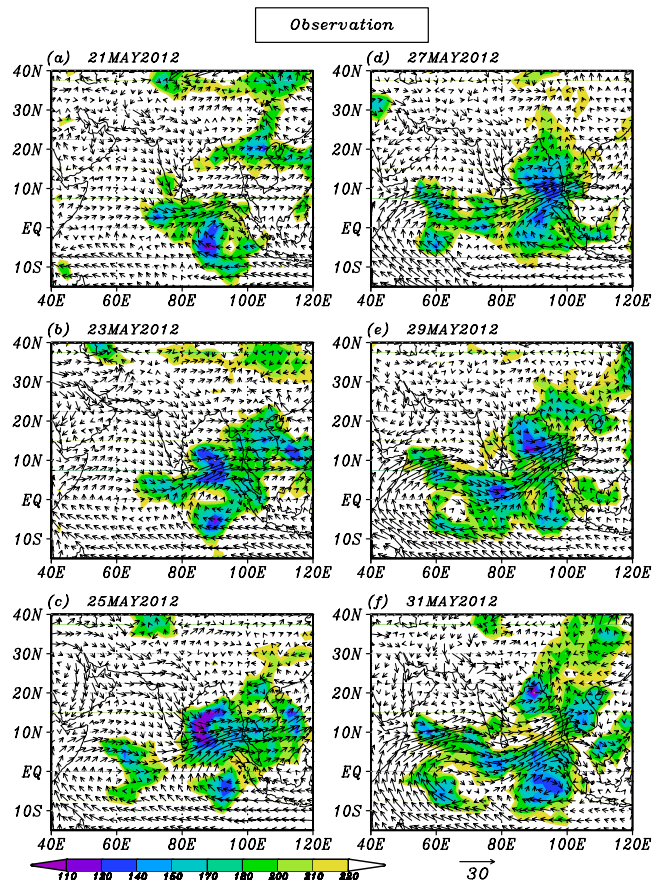


Fig. 2. Outgoing longwave radiation (OLR) [W m^{-2}] and 850-hPa wind circulation field [m s^{-1}] from (a) 21 May, 2012 to (f) 31 May, 2012 during ISM onset process in observations.

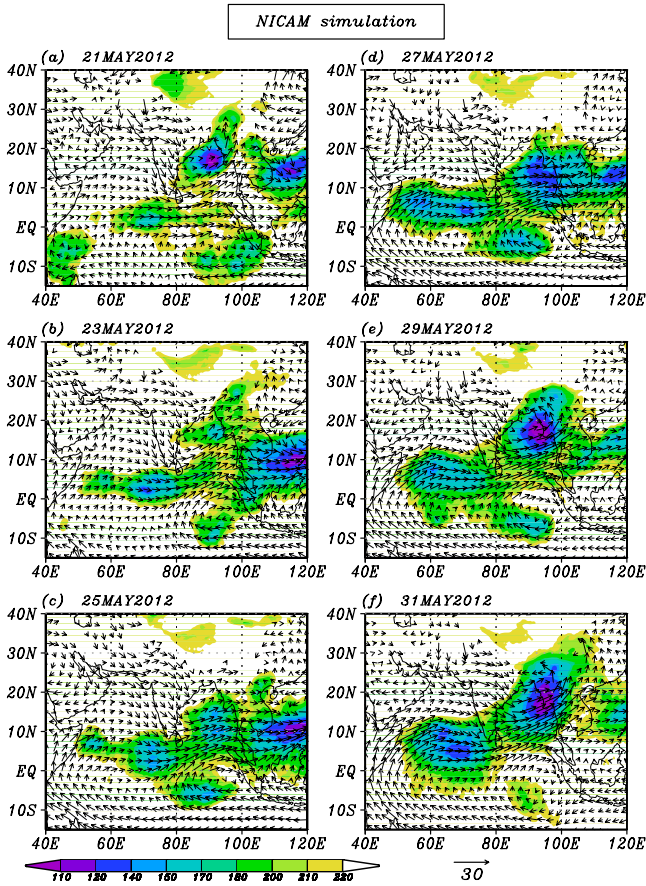


Fig. 3. Same as Fig. 2 except for the NICAM simulations averaging five runs with different initial conditions from 15–19 May.

low-level convergence along the Western Ghats with westerly flow over the Indian sub-continent. This convection, accompanied by the tropical disturbances over the Bay of Bengal, most likely triggered ISM onset in 2012.

Figure 3 shows NICAM simulation data similar to those shown in Fig. 2. Although strong convection was prominent over the South China Sea by 27 May in the simulations, which differed from observational findings, the five-member ensemble simulation results show symmetric convection of two cyclonic circulations over the northern and southern hemispheres along the 90°E gridline on 21 May. The convection with cyclonic circulation over the southern hemisphere in the simulations became weaker than that observed; however, the tropical disturbance over the Bay of Bengal moved northward and ISM onset occurred in early June. The NICAM simulations of the tropical disturbances were in good

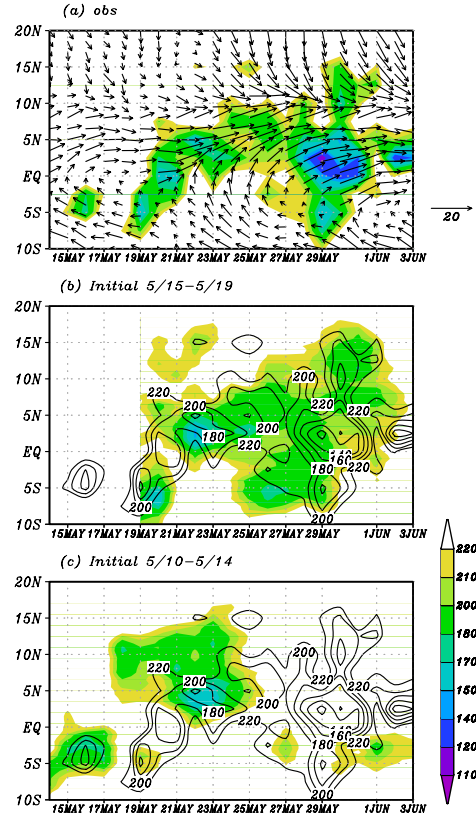


Fig. 5. (Top) OLR [$W m^{-2}$] and 850-hPa wind [$m s^{-1}$] averaging 85°E–95°E in observations. (Middle) OLR of NICAM simulations averaging five runs with different initial conditions from 15–19 May (shading), with observational OLR (contour) superimposed. (Bottom) Same as the Middle, but averaging five runs with different initial conditions from 10–14 May.

agreement with observations, including ISM onset prediction, with a lead time of approximately two weeks.

On the other hand, it should be noted that the development of convection in northern and southern hemisphere is different between NICAM simulations and observations. More developed convection over the northern convection and less developed over the southern convection in the simulations modified the monsoon westerly over the Bay of Bengal. As a result, the meridional shear of zonal wind (ISM index) became weak. This corresponds to small value of ISM index in the middle of June after the onset (Fig. 1).

To highlight the effect of being able to reproduce the tropical disturbances accurately in ISM onset simulations, Figs. 4 and 5 show a Hovmöller diagram of the OLR along the equator and 80°E in observation and two different ensemble composites: one

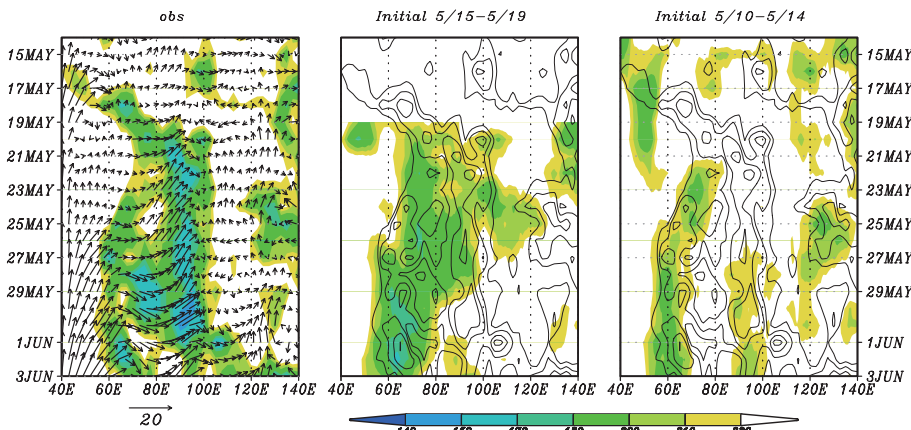


Fig. 4. (Left) OLR [$W m^{-2}$] and 850-hPa wind [$m s^{-1}$] averaging 5°S–5°N in observations. (Middle) OLR of NICAM simulations averaging five runs with different initial conditions from 15–19 May (shading), with observational OLR (contour) superimposed. (Right) Same as the Middle, but averaging five runs with different initial conditions from 10–14 May.

that corresponds to the average of the simulations initialized from 15 May to 19 May as the most realistic ISM onset simulation, and the other as the average from 10 May to 14 May. Note that the latter ensemble composite fails to capture the actual ISM onset process (Fig. 1). In the observations, over the period from 18–26 May the active convection moved significantly eastward, from 70°E to 120°E. The former ensemble composite captured the eastward-propagating convection, although the convection over the western Pacific was much weaker, whereas the latter did not show a clear signal over the Indian Ocean corresponding to the 21 May data, and eastward-moving convection was not detected. After the eastward-propagating convection reached the eastern Indian Ocean, the northward moving convection was formed in the observations and former ensemble composite. That convection was not reproduced in the latter ensemble due to the failure of the eastward propagating convection. Hence, the ability to reproduce the tropical disturbance over the equatorial Indian Ocean and the Bay of Bengal was strongly correlated with ISM onset behavior in simulations.

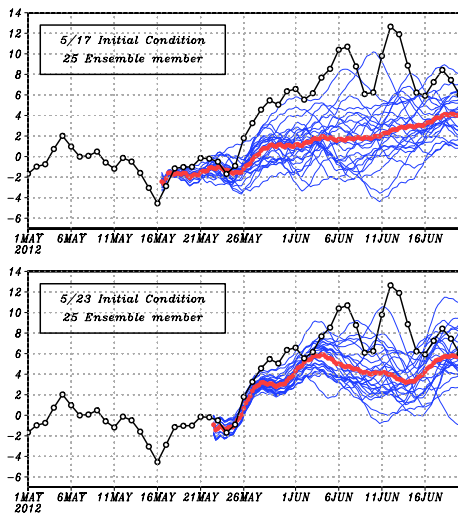


Fig. 6. Time series of the ISM index in the operational ensemble prediction system extended-range forecasting of JMA with initial data from 17 May (Top) and 23 May (Bottom).

4. Comparison with the JMA ensemble prediction system

Here, we compared the NICAM simulations with the JMA EPS forecast to evaluate the performance. Figure 6 shows time series of the ensemble mean ISM indices of the JMA EPS initialized at 17 May and 23 May. The ensemble mean starting on 17 May fails to capture the abrupt ISM onset, showing instead a gradual increase in the ISM index. This signifies that the axis of the westerly monsoon gradually moved northward. The simulations starting on 23 May capture the abrupt ISM onset well, in addition to the northward moving tropical disturbances over the Bay of Bengal (figure not shown). The difference between the two results should be evident in the signal corresponding to the initial conditions, deemed to be the seed of the eastward-propagating tropical disturbance.

Figure 7 shows the observational conditions on 17 May and 23 May and the ensemble simulation results starting on 17 May from the JMA EPS. A vertical velocity at 500 hPa was assumed as an alternative for OLR in the JMA EPS results (Figs. 7c, d, e). The difference in the observational evidence between 17 May and 23 May shows the robustness of the convection over the Indian Ocean. The convection associated with the eastward-propagating tropical disturbance over the western Indian Ocean was still weaker on 17 May. The JMA EPS results from 17 May show relatively weak convection (upward motion) over the equatorial Indian Ocean during late May, followed by gradual movement northward, which contributed to westerly flow over the Indian sub-continent later than that observed. In contrast, based on the 17 May data, NICAM simulated the eastward-propagating convection along the equatorial Indian Ocean and reproduced the tropical disturbance that induced ISM onset in early June (Fig. 3).

5. Concluding remarks and discussion

The onset of ISM signifies the commencement of the rainy season in south-southeastern Asia, with an abrupt change in large-scale atmospheric circulations. Although the interannual variability in the timing of ISM onset strongly affects the broad Asian monsoon area, the ability to predict monsoon onset accurately remains a challenge owing to the short lead time. In this study, we investigated the onset processes of ISM in 2012 and discussed the

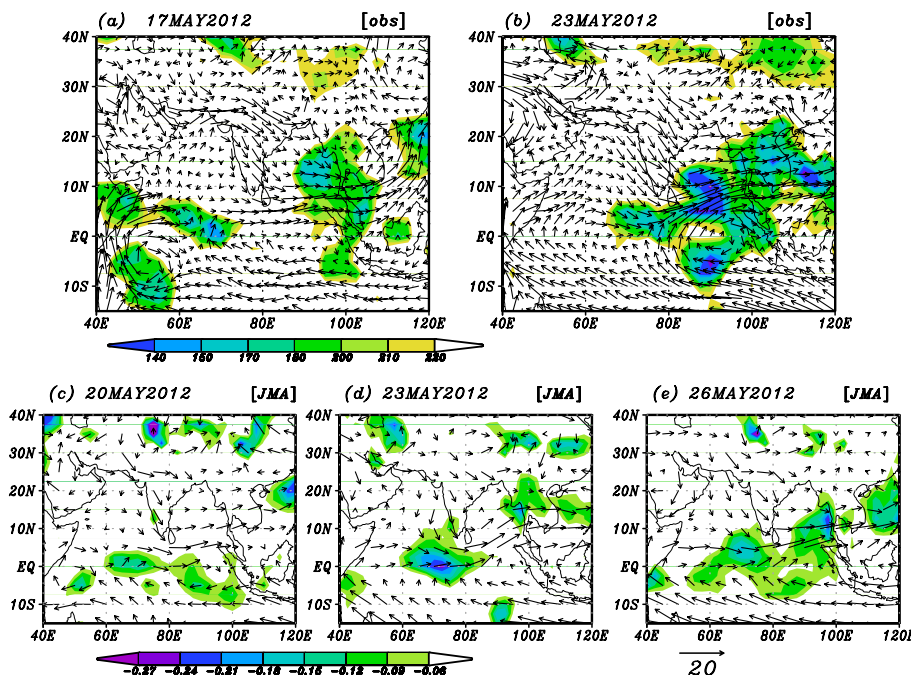


Fig. 7. OLR [W m^{-2}] and 850-hPa wind field [m s^{-1}] in observations for (a) 17 May and (b) 23 May. Vertical wind speed at 500-hPa and 850-hPa wind fields of the ensemble simulation of JMA EPS on (c) 20 May, (d) 23 May, and (e) 26 May, initialized on 17 May.

potential of extended forecasting by using a global cloud-system resolving model, which has the advantage of more accurate simulation of tropical disturbances.

In 2012, ISM onset was announced on 5 June. A series of NICAM experiments with 14-km horizontal resolution was performed with various initial conditions. NICAM demonstrated excellent performance in providing a realistic simulation of abrupt ISM onset, with northward-migrating tropical disturbances over the Bay of Bengal and the Arabian Sea during late May. The earliest initial date for accurate ISM onset simulations using NICAM was 15 May, whereas the JMA operational EPS (1-month duration) did not capture the abrupt ISM onset given the initial conditions of 17 May. In a comparison with JMA EPS, the better reproducibility of the tropical disturbances seen with the NICAM-based model extended the predictability of the transition phase for the Asian summer monsoon. When the model failed to reproduce the eastward-propagating tropical disturbance along the equatorial Indian Ocean, the simulated ISM did not have an abrupt onset but instead developed gradually in both the NICAM and JMA EPS simulations.

The development of tropical disturbances over the central Indian Ocean and Bay of Bengal was a key phenomenon for better simulation of ISM onset in 2012. This tropical disturbance over the Bay of Bengal was accompanied by the eastward-propagating convections. Thus, better reproduction of the tropical disturbance over the Indian Ocean in models should enhance their potential to extend the predictability of the transition phase for the Asian summer monsoon. Less accurate reproducibility of the tropical disturbances in simulations may result in gradual northward movement of the monsoon westerly winds, and hence a delay in ISM onset compared with observations. Thus, these results provide insight into improving the predictability of monsoon onset using the global model (Sperber et al. 2013). We suggest that global cloud-system resolving models without convective parameterization have potential to better simulation of ISM, as similar result to the MJO simulations (Holloway et al. 2013)

The underlying triggering mechanism and the interaction between tropical disturbances and large-scale monsoon onset are still under discussion. NICAM was used as an atmosphere-only GCM in this study; however, air–sea interactions may provide additional information on ISM onset with the tropical disturbances. Questions remain regarding the physical mechanisms of this interaction. Additionally, WNPM onset is difficult to simulate more than 1 week in advance. Climatologically, WNPM onset is two weeks earlier than that of ISM. Failure to simulate WNPM onset realistically may limit extension of ISM onset predictability. Thus, the relationship between ISM and WNPM is an interesting topic for future work.

Acknowledgements

The authors are grateful to Dr. Masato Sugi, the editor of the SOLA, and anonymous reviewers for their useful comments. Special thanks are due to Prof. Bin Wang in IPRC, University of Hawaii for lots of useful comments. This work is supported by RIKEN Incentive Research Projects 2014 and MEXT Strategic Programs for Innovative Research (SPIRE). This work also has been done by using the K computer at the RIKEN AICS (Proposal number hp120313).

References:

Fudeyasu, H., Y. Q. Wang, M. Satoh, T. Nasuno, H. Miura, and W. Yanase, 2008: Global cloud-system-resolving model NICAM successfully simulated the lifecycles of two real tropical cyclones. *Geophys. Res. Lett.*, **35**, L22808, doi:10.1029/2008gl036003.

Gadgil, S., and K. Rupa Kumar, 2006: The Asian monsoon – agriculture and economy. *The Asian Monsoon*, B. Wang, Ed., Praxis Publishing Ltd, 651–683.

Holloway, C. E., S. J. Woolnough, and G. M. S. Lister, 2013: The effects of explicit versus parameterized convection on the MJO in a large-domain high-resolution tropical case study. Part I: Characterization of large-scale organization and propagation. *J. Atmos. Sci.*, **70**, 1342–1369.

Hung, C.-W., and M. Yanai, 2004: Factors contributing to the onset of the Australian summer monsoon. *Quart. J. Roy. Meteor. Soc.*, **130**, 739–758.

Joseph, P. V., J. K. Eischeid, and R. J. Pyle, 1994: Interannual variability of the onset of the Indian-summer monsoon and its association with atmospheric features, El-Nino, and sea-surface temperature anomalies. *J. Climate*, **7**, 81–105.

Joseph, P. V., K. P. Sooraj, and C. K. Rajan, 2006: The summer monsoon onset process over South Asia and an objective method for the date of monsoon onset over Kerala. *Int. J. Climatol.*, **26**, 1871–1893.

Kikuchi, K., B. Wang, and Y. Kajikawa, 2012: Bimodal representation of the tropical intraseasonal oscillation. *Climate Dyn.*, **38**, 1989–2000.

Kirtman, B. P., and J. Shukla, 2000: Influence of the Indian summer monsoon on ENSO. *Quart. J. Roy. Meteor. Soc.*, **126**, 213–239.

Li, J. P., and L. Zhang, 2009: Wind onset and withdrawal of Asian summer monsoon and their simulated performance in AMIP models. *Climate Dyn.*, **32**, 935–968.

Liebmann, B., and C. A. Smith, 1996: Description of a complete (interpolated) outgoing longwave radiation dataset. *Bull. Amer. Meteor. Soc.*, **77**, 1275–1277.

Miura, H., M. Satoh, T. Nasuno, A. T. Noda, and K. Oouchi, 2007: A Madden-Julian Oscillation event realistically simulated by a global cloud-resolving model. *Science*, **318**, 1763–1765.

Miyakawa, T., and co-authors, 2014: Madden-Julian Oscillation prediction skill of a new-generation global model demonstrated using a supercomputer. *Nature Commun.*, **5**, 3769, doi:10.1038/Ncomms4769.

Moron, V., and A. W. Robertson, 2014: Interannual variability of Indian summer monsoon rainfall onset date at local scale. *Int. J. Climatol.*, **34**, 1050–1061.

Nakano, M., M. Sawada, T. Nasuno, and M. Satoh, 2015: Intraseasonal variability and tropical cyclogenesis in the western North Pacific simulated by a global nonhydrostatic atmospheric model. *Geophys. Res. Lett.*, **42**, doi:10.1002/2014GL062479.

Onogi, K., and co-authors, 2007: The JRA-25 reanalysis. *J. Meteorol. Soc. Japan*, **85**, 369–432.

Oouchi, K., A. T. Noda, M. Satoh, B. Wang, S. P. Xie, H. G. Takahashi, and T. Yasunari, 2009: Asian summer monsoon simulated by a global cloud-system-resolving model: Diurnal to intra-seasonal variability. *Geophys. Res. Lett.*, **36**, L11815, doi:10.1029/2009gl038271.

Reynolds, R. W., N. A. Rayner, T. M. Smith, D. C. Stokes, and W. Q. Wang, 2002: An improved in situ and satellite SST analysis for climate. *J. Climate*, **15**, 1609–1625.

Satoh, M., T. Matsuno, H. Tomita, H. Miura, T. Nasuno, and S. Iga, 2008: Nonhydrostatic icosahedral atmospheric model (NICAM) for global cloud resolving simulations. *J. Comput. Phys.*, **227**, 3486–3514.

Satoh, M., and co-authors, 2014: The Non-hydrostatic Icosahedral Atmospheric Model: Description and Development. *Prog. Earth Planet. Sci.*, **1**(18), doi:10.1186/s40645-014-0018-1.

Sperber, K., and co-authors, 2013: The Asian summer monsoon: An intercomparison of CMIP5 vs. CMIP3 simulations of the late 20th century. *Climate Dyn.*, **41**, 2711–2744.

Subrahmanyam, M. V., B. Pushpanjali, and K. P. R. V. Murthy, 2013: Indian summer monsoon onset variations and consecutive rainfall over India. *Ecol. Environ. Conserv.*, **19**, 595–599.

Tomita, H., and M. Satoh, 2004: A new dynamical framework of non-hydrostatic global model using the icosahedral grid. *Fluid Dyn. Res.*, **34**, 357–400.

Wang, B., R. G. Wu, and K. M. Lau, 2001: Interannual variability of the Asian summer monsoon: Contrasts between the Indian and the western North Pacific-east Asian monsoons. *J. Climate*, **14**, 4073–4090.

Yamaura, T., Y. Kajikawa, H. Tomita, and M. Satoh, 2013: Possible impact of a tropical cyclone on the northward migration of the Baiu frontal zone. *SOLA*, **9**, 89–93.